Weak Localization of Photons: Termination of Coherent Random Walks by Absorption and Confined Geometry

S. Etemad, R. Thompson, and M. J. Andrejco
Bell Communications Research, Red Bank, New Jersey 07701

and

Sajeev John and F. C. MacKintosh
Department of Physics, Princeton University, Princeton, New Jersey 08540
(Received 6 May 1987)

We compare the effects of finite thickness and absorption on the line shape of the coherent backscattering peak from a disordered medium. By termination of the coherent random walk of photons through confined geometry and/or absorption, contributions of different time-reversed paths to the line shape of the backscattering peak have been determined. Using circularly polarized light, we find good agreement between the experimental and calculated line shape of the helicity-preserving channel whose coherent backscattering peak closely resembles that of a scalar field.

PACS numbers: 42.20.−y, 71.55.Jv

Propagation of coherent waves through disordered media possesses peculiarities that are direct consequences of the retention of the phase memory. For example, electronic transport through a structure smaller than the *inelastic*-scattering length can no longer be viewed as diffusive propagation of a classical particle. As a result, conductance of such a small structure is dominated by *wave-mechanical* corrections which are interference effects caused by the coherent state of the electron. Such wave-mechanical corrections have been a subject to extensive studies in the contexts of weak localization of electrons, Aharanov-Bohm effect, and universal conductance fluctuations.[1-3] Weak localization, whose origin lies in the phenomenon of coherent backscattering, is of fundamental importance because it is the precursor to the occurrence of a true mobility edge and the Anderson localization transition.[4,5]

In the presence of time-reversal symmetry, the weak-localization effect arises from a constructive interference between two amplitudes of a coherent wave traveling the same path in the opposite directions, and arriving at the backscattering direction with the same phase.[1] In the case of electronic transport, this effect gives rise to enhanced resistance. Application of a magnetic field breaks the time-reversal symmetry and leads to a large negative magnetoresistance that is attributed to the weak localization of electrons.[2] Recently the analogy between the weak localization of electrons, as a wave phenomenon, and of photons which are inherently wavelike has been emphasized.[6-9] The enhanced resistance associated with the weak localization of photons appears as a sharp peak in the backscattering direction.[10] The backscattering peak is found only after ensemble averaging of the large, sample-specific fluctuations that originate from interference effects due to multiple scattering of the wave inside the bulk.[8] The height of the backscattering peak is twice the average scattering intensity, since in the backscattering direction, there is complete constructive interference. In other words, the square of the sum of two in-phase amplitudes is *exactly twice* the sum of the squares of the amplitudes. The width of the peak is of the order of λ/l, where λ is the wavelength of the light and l is the *elastic*-scattering length.

In this Letter we present a joint experimental and theoretical study of the line shape of the coherent backscattering peak for light and its dependence on the various time-reversed paths. To map out the contributions to the backscattering peak from different paths, we selectively terminate the coherent random walks through two means: confined geometry and elimination by absorption. In the confined-geometry studies, we monitor the depth that a path can penetrate through the medium by simply varying the thickness of the medium; i.e., for any path that extends beyond the thickness of the medium, the photon is transmitted and does not contribute to the backscattering peak. In the absorption studies, we eliminate those photons that took paths longer than the absorption length, and remove their contribution to the backscattering peak. Although both absorption and confined geometry terminate a coherent random walk in similar manners, their effects on the line shape show a subtle difference which is attributed to the difference between the deterministic and probabilistic natures of the two means, respectively. These results are obtained by projecting out the circularly polarized components of the incident and reflected waves. For this helicity-preserving channel, we find that the observed peak line shapes are in close agreement with those obtained for scalar waves. Such identification does not occur for linearly polarized light.

The setup for the backscattering experiment is similar to the one we used in our previous study.[8] The signal-

to-noise ratio has been improved considerably as a result of placing the chopper used for the phase-sensitive detection between the "isolator" and the sample. Unless otherwise stated, the coherent radiation used for the results reported here is the 514-nm line from an argon-ion laser. In all traces we have used the isolator, which we originally designed to eliminate the contribution from uninteresting single-scattering events.[8] As described in the theoretical analysis, the use of the isolator, which is a combination of a linear polarizer followed by a $\lambda/4$ plate, enables us to probe the helicity-preserving part of the backscattering intensity.

The medium for the confined-geometry studies is a connected network of colloidal silica particles in air described in our earlier work.[8] Uniform-thickness slabs are deposited directly on quartz discs by flame hydrolysis of silicon tetrachloride vapor. We can vary w, the thickness of the medium, from a few microns to a few millimeters, covering the full range from $w \simeq l$ to $w \gg l$. The thicknesses of these slabs are determined with an optical microscope to within a few microns. To form an ensemble average of the sample-specific fluctuations in the backscattering intensity,[8] we move the sample rapidly in the beam by spinning the quartz disc substrate on a second chopper. The result is a smooth backscattering peak with details that are limited by the resolution of the diffractometer. Because of the high purity of the silica beads we find no evidence for absorption effects in these studies.

In Fig. 1 we show the backscattering results from four slabs of different thicknesses. The absolute intensity of the backscattering peak is in the same unit for all curves. The zero level for the intensity has been adjusted so that all curves have the same scattering intensity for angles far away from the backscattering direction. These results are from a more extensive set of samples that all nest equally well under the peak obtained from the 1000-μm-thick slab, which is effectively an infinitely thick medium. The rest of these results are not shown for clarity of the presentation. The enhancement factor at exactly the backscattering direction is about a factor of 2 for all curves except where the resolution of the diffractometer ($\simeq$0.6 mrad) rounds off the sharp peak. The open circles are the theoretical fit to these results that is described later on. We note that qualitatively similar finite-size effects have been observed for linearly polarized light[11]; however, the factor of 2 enhancement in exactly the backscattering direction is not observed.[12]

To study the effect of absorption on the line shape of the backscattering peak, we resort to a colloidal suspension of polystyrene balls in water similar to those used in the earlier studies.[6-8] By dissolving rhodamine 6G dye in the water which contains the polyballs, we make a red cloudy mixture. *Using the 633-nm radiation from a He-Ne laser, we find no detectable difference in the intensity and line shape of the backscattering peaks obtained from this red mixture and from the original white polyball suspension.* To measure the absorption coefficient, we dissolve the same amount of dye in pure water. In agreement with the above finding, there is no detectable absorption ($\alpha \ll 1$ cm^{-1}) of the 633-nm radiation by the dye solution. However, the same solution attenuates the 514-nm radiation without any detectable scattering effect. We can vary the absorption coefficient, α, from nonabsorbing up to $\alpha \cong 100$ cm^{-1}. For the case of ballistic propagation, we may identify the inelastic mean free path as $l_{\text{inel}} = \alpha^{-1}$.

In Fig. 2 we compare the backscattering peak from two scattering media of the same l: a polyball suspension in dyed water that has $l_{\text{inel}} = 400$ μm and a nonabsorbing one. The absolute intensity scale for both curves is the same. As in the results of Fig. 1, we have adjusted

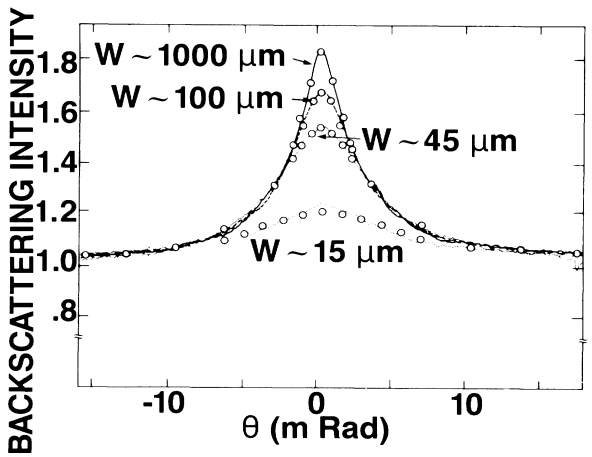

FIG. 1. A deterministic means of terminating a coherent random walk: The effect of confined geometry on the line shape of the backscattering peak, where the elastic scattering length is $l \cong 11$ μm and w is the thickness of the medium.

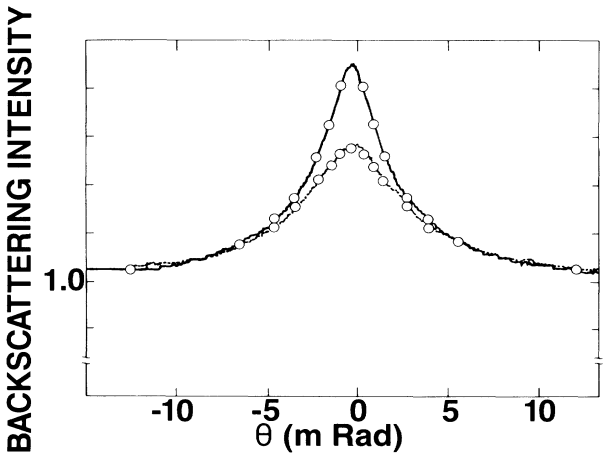

FIG. 2. A probabilistic means of terminating a coherent random walk: The effect of absorption on the line shape of the backscattering peak, where $l \cong 13$ μm for both the nonabsorbing and absorbing ($\alpha^{-1} \cong 400$ μm) media.

the zero intensity level so that the scattering intensities from the two media are the same in the wings. The curves from polyball suspensions with intermediate absorption constants nest between the results shown in Fig. 2. The open circles are again the theoretical fits to the results.

As seen in the results shown in Figs. 1 and 2, the effects of both finite thickness and absorption on the coherent backscattering peak are similar, provided we make the identification

$$w \cong (l l_{\text{inel}}/3)^{1/2}. \tag{1}$$

This is because both effects tend to remove the contributions of the longer time-reversed paths to the coherent backscattering peak. To see this effect qualitatively, consider two time-reversed paths with N elastic-scattering events. Figure 3 is a schematic diagram of such a case in $\mathbf{k}$ space, where we have illustrated the case for $N=3$. In the two time-reversed paths, $\mathbf{k}_i \rightarrow \mathbf{k}_2 \rightarrow \mathbf{k}_3 \rightarrow \mathbf{k}_f$ and $\mathbf{k}_i \rightarrow -\mathbf{k}_2' \rightarrow -\mathbf{k}_3' \rightarrow \mathbf{k}_f$, $\mathbf{k}_i$ is the initial wave vector and $\mathbf{k}_f$ is the final wave vector. They describe a photon being backscattered from k_i to k_f through intermediate (virtual) states $\mathbf{k}_2, \mathbf{k}_3$ and $-\mathbf{k}_2', -\mathbf{k}_3'$, respectively, *by the same sequence of wave-vector transfers* $\mathbf{g}_1, \mathbf{g}_2, \mathbf{g}_3$. If $\mathbf{q} \equiv \mathbf{k}_i + \mathbf{k}_f = 0$, then the corresponding intermediate states $\mathbf{k}_n'$ and $-\mathbf{k}_n'$ match each other in $|k|$, hence in frequency, and there is constructive interference between the two amplitudes. If, on the other hand, we consider backscattering into a direction for which $q \neq 0$, then the corresponding intermediate states no longer coincide in frequency with their partners. For small q, the associated frequency difference for the nth pair is $\delta\omega_n = c(\mathbf{q} \cdot \hat{\mathbf{k}}_n)$. This is allowed because of the smearing of the energy shell by an amount $c\delta k \simeq c/l$; i.e., the intermediate states are not well defined within the time scale of τ, where $\tau = l/c$ is the elastic mean free time. The incurred phase difference between each of the nth corresponding pairs in the two time-reversed paths is $\delta\phi_n = \delta\omega_n \tau$. Since the direction of $\hat{\mathbf{k}}_n$ of the intermediate states is a random variable, it follows that the accumulated phase difference is $\Delta\phi = \sqrt{N}\delta\phi_{\text{rms}}$, where the root mean square phase difference can be shown to be $\delta\phi_{\text{rms}} \equiv \langle |\delta\omega_n \tau|^2 \rangle_{\text{av}}^{1/2} = ql/\sqrt{3}$. The factor $1/\sqrt{3}$ comes from the three-dimensional averaging of the square of the cosine of the angle between $\mathbf{q}$ and $\hat{\mathbf{k}}_n$. The condition for constructive interference is then given by

$$\Delta\phi = lq(N/3)^{1/2} \leq 1. \tag{2}$$

It follows that only those paths of length $N \leq 3/(ql)^2$ contribute to the coherent intensity for angles $\theta \geq q/k$ away from the direction of $-k_i$.

The similarity of the results shown in Figs. 1 and 2 is now readily explained. The confined geometry (slab of thickness w) leads to an elimination of paths of length $N \geq 3(w/l)^2$ and the absorption likewise leads to elimination of paths of length $N \geq l_{\text{inel}}/l$. It follows that for a finite-thickness slab, backscattering into angles $\theta \geq l/kw$ is essentially unaffected and that for absorption the same is *approximately* true for angles $\theta \geq (1/k) \times (3/l_{\text{inel}}l)^{1/2}$ (see Figs. 1 and 2).

The line shapes obtained for linearly polarized incident light backscattered into either the parallel or perpendicular polarization differ from those obtained for scalar waves.[11-15] Our calculation of the backscattering line shape, however, shows that for circularly polarized light, the line shape of the helicity-preserving channel closely resembles that of a scalar wave.[16] These calculations are performed in a diffusion approximation, within a white-noise model for the fluctuating dielectric constant with a generalization of the Green's-function technique introduced by Stephen and Cwilich.[14] We find, from fitting the experimental results, the boundary conditions that the diffusion propagator vanishes on trapping planes located a distance $0.7l$ from either surface of the slab.[16]

Experimentally, our use of the isolator (a linear polarizer followed by a $\lambda/4$ plate) enables us to probe this helicity-preserving part of the coherent backscattering peak. In the first passage through the isolator, the incident beam is circularly polarized. In the second passage, the multiply scattered light is passed through to the detector only if it has *the same circular polarization.* The backscattering peaks shown in Figs. 1 and 2 are, therefore, representative of multiple scattering into a helicity-preserving channel.

To fit the experimental results shown in Fig. 1, we first fit the scattering intensity from the 1000-μm-thick slab, which is effectively an infinite medium, using the known resolution of the diffractometer. This fit is shown as open circles. The single variable used for this fit is the elastic-scattering length, l. From this fit we obtain a value of $l = 11$ μm. This is in good agreement with a value of $l = 10 \pm 1$ μm obtained by measurement of the

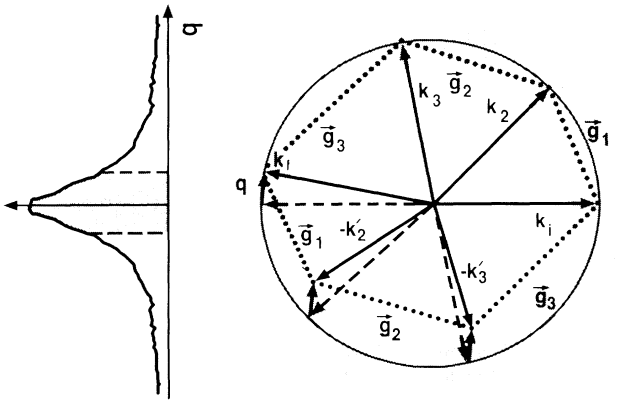

FIG. 3. Construction of coherent backscattering peak from time-reversed paths shown in k space. The two actual paths shown are for three scattering events.

coherent, direct transmission of the laser beam through samples of different thickness, which is expected to vary as $\exp(-w/l)$.[8] Now we can fit the scattering intensities from finite-thickness slabs with no adjustable parameter. For the thinnest slab ($w \simeq 15$ μm) the fit is less accurate. This most likely arises from a breakdown of the diffusion approximation.[12] The absorption results shown in Fig. 2 have also been fitted in a similar manner. That is, we first obtained the value of l by fitting the line shape of the nonabsorbing medium. This fit, shown as open circles in Fig. 2, is obtained with $l = 13$ μm, a value consistent with the previous measurements.[6,7] The absorption effect is now fitted with no adjustable parameter with the value of $l_{\text{inel}} \cong 400$ μm.

The high quality of the experimental line shapes presented here allows us to see an interesting difference between confined-geometry and absorption effects for angles $\theta > (1/k)(3/l_{\text{inel}}l)^{1/2}$. A detailed comparison between finite slab thickness and absorption effects reveals that in the former case the wings of the backscattering peak are completely unaffected, whereas in the latter case there is a slight decrease of the coherent intensity even for angles $\theta \geq (1/k)(3/l_{\text{inel}}l)^{1/2}$. These slight differences arise from the fact that there is a nonzero probability of absorption for arbitrarily short paths, whereas only those paths long enough to traverse the slab thickness are affected by the confined geometry. This subtle difference is evident in the experimental results if we use Eq. (1) to identify the slab thickness "comparable" to l_{inel}. Using $l \cong 11$ μm and $l_{\text{inel}} \cong 400$ μm, we obtain $w_{\text{comp}} \cong 38$ μm. In other words, the curve in Fig. 1 with $w \cong 45$ μm should be chosen for comparison with the absorption result of Fig. 2. As we can see, suppression of the peak intensity for both curves is roughly the same. However, for θ between 3 and 5 mrad, the absorption curve is noticeably more suppressed as a result of this expected difference between the deterministic and probabilistic means of terminating a coherent random walk.

In summary, we have found quantitative agreement between theory and experiment for the helicity-preserving channel of the coherent backscattering peak line shape from a disordered medium. By terminating the coherent random walk of photons through either confined geometry or absorption, we have determined contributions of different time-reversed paths to the line shape of the backscattering peak.

[1]D. E. Khmel'nitskii, Physica (Amsterdam) **126B**, 235 (1984).

[2]G. Bergmann, Phys. Rep. **107**, 1 (1984).

[3]P. A. Lee and A. D. Stone, Phys. Rev. Lett. **55**, 1622 (1985).

[4]S. John, Phys. Rev. Lett. **53**, 2169 (1984).

[5]P. W. Anderson, Philos. Mag. B **52**, 505 (1985).

[6]M. P. van Albeda and A. Lagendijk, Phys. Rev. Lett. **55**, 2692 (1985).

[7]P. E. Wolf and G. Maret, Phys. Rev. Lett. **55**, 2696 (1985).

[8]S. Etemad, R. Thompson, and M. J. Andrejco, Phys. Rev. Lett. **57**, 575 (1986).

[9]M. Kaveh, M. Rosenbluh, I. Edrei, and I. Freund, Phys. Rev. Lett. **57**, 2049 (1986).

[10]Y. Kuga and A. Ishimaru, J. Opt. Soc. Am. A **1**, 831 (1984).

[11]M. P. van Albada, M. B. van der Mark, and Ad Lagendijk, Phys. Rev. Lett. **58**, 361 (1987).

[12]M. B. van der Mark, M. P. van Albada, and Ad Lagendijk, to be published.

[13]S. Etemad, to be published.

[14]M. J. Stephen and G. Cwilich, Phys. Rev. B **34**, 7564 (1986).

[15]E. Akkermans, P. E. Wolf, and R. Maynard, Phys. Rev. Lett. **56**, 1471 (1986).

[16]F. MacKintosh and S. John, Phys. Rev. B (to be published).

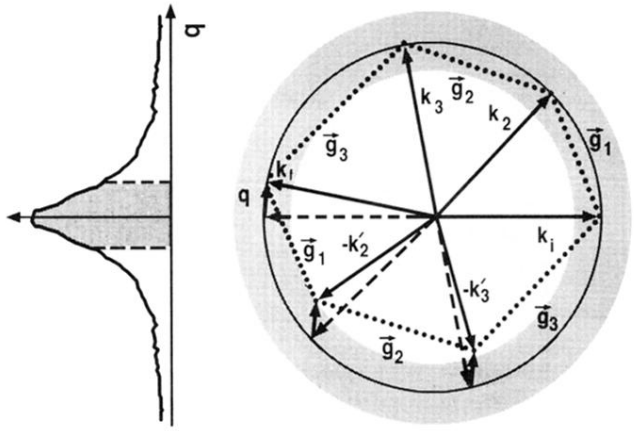

FIG. 3. Construction of coherent backscattering peak from time-reversed paths shown in k space. The two actual paths shown are for three scattering events.